

# Structural and Optical Characterization of Silica@PbS Core–Shell Nanoparticles

A. Pourahmad, Sh. Gharipour

**Abstract**—The present work describes the preparation and characterization of nanosized SiO<sub>2</sub>@PbS core-shell particles by using a simple wet chemical route. This method utilizes silica spheres formation followed by successive ionic layer adsorption and reaction method assisted lead sulphide shell layer formation. The final product was characterized by X-ray diffraction (XRD), scanning electron microscopy (SEM), UV–vis spectroscopic, infrared spectroscopy (IR) and transmission electron microscopy (TEM) experiments. The morphological studies revealed the uniformity in size distribution with core size of 250 nm and shell thickness of 18 nm. The electron microscopic images also indicate the irregular morphology of lead sulphide shell layer. The structural studies indicate the face-centered cubic system of PbS shell with no other trace for impurities in the crystal structure.

**Keywords**—Core-shell, nanostructure, semiconductor, optical property, XRD.

## I. INTRODUCTION

RECENTLY, much interest was aroused in synthesis of semiconducting nanoparticles intended for application in modern microelectronic devices. The possibility of producing semiconducting nanoparticles with controllable size and shape is being extensively studied [1]–[4]. The interest in lead sulphide PbS as one of numerous semiconducting materials is due not only to its properties (a narrow forbidden gap of ~0.41 eV and a large size of exciton, ~18–24 nm), but also to its diverse morphology, which changes when different reactants or synthesis methods are used. PbS has been widely used in many fields such as Pb<sup>2+</sup> ion selective sensor, IR detectors, solar absorber and photography [5]. Nanoparticles of lead sulphide have been synthesized recently by different chemical methods with the controlled particle size distribution [6], [7]. Preparation of nano-architecture core-shell structures is a potentially effective method to solve the problems associated with volume expansion. Core–shell type of geometry is of particular interest and core–shell materials offer potential applications in electrical and optical materials, magnetic materials, and bio-environmental materials. A shell structural domain covering a core domain constitutes the core–shell materials and the starting materials for the two domains can be metallic, ceramic, or polymeric materials [8], [9]. In the present report, we present the synthesis of SiO<sub>2</sub>@PbS nanostructure material by using a simple and reliable process.

A. Pourahmad is with the Department of Chemistry, Rasht Branch, Islamic Azad University, Rasht, Iran (corresponding author; phone: ++98 13 33110721; fax: ++98 1333424094; e-mail: pourahmad@iaurasht.ac.ir).

Sh. Gharipour is with the Department of Chemistry, Rasht Branch, Islamic Azad University, Rasht, Iran (e-mail: shiva.gharipour@gmail.com).

## II. MATERIALS AND METHODS

### A. Synthesis of SiO<sub>2</sub>@PbS Nanoparticles

All the chemical reagents were commercial with analytical grade purity, and used directly without further purifications. We followed the Stober process of silica particle synthesis. In a typical synthesis, cetyltrimethylammonium bromide (CTAB) of 0.5 g, ammonia solution of 30 ml and ethanol of 80 ml were mixed in 100 ml of water. Then, 600 µl of tetra ethyl orthosilicate have been added. After 1 h the white powders were collected by centrifugation and dispersed in lead acetate (0.3 g in 100 ml) solution. After 5 min, the powders were collected back by centrifugation and then washed with water. Then, dispersed again in the sodium sulphide solution (0.3 g in 100 ml) and then collected back for drying. The dried powder was directly taken into further characterizations.

### B. Characterization

Powder XRD patterns of the samples were recorded using an X-ray diffractometer (Bruker D8 Advance) with Co K $\alpha$  radiation ( $\lambda = 1.789 \text{ \AA}$ ) under the conditions of 40 kV and 30 mA, at a step size of  $2\theta = 0.02^\circ$ . The UV–Vis diffused reflectance spectra (UV–Vis DRS) obtained from UV–Vis Scinco 4100 spectrometer with an integrating sphere reflectance accessory. BaSO<sub>4</sub> was used as reference. The infrared spectra on KBr pellet were measured on a Bruker spectrophotometer. The transmission electron micrographs (TEM) were recorded with a Philips CM10 microscope, working at a 100 kV accelerating voltage. Samples for TEM were prepared by dispersing the powdered sample in acetone by sonication and then drip drying on a copper grid coated with carbon film. The surface morphology of the samples was obtained using a Jeol-JSM-5610 LV SEM.

## III. RESULTS AND DISCUSSION

The liquid crystal templating has been used here for the formation of SiO<sub>2</sub> spheres then SILAR assisted PbS shell layer is formed over the SiO<sub>2</sub> spheres. At first, the CTAB micelles are formed above the critical micelle concentration. Then silicate ions are precipitating over the head groups of CTAB due to complementary of charges. After this, hydrolysis followed by condensation of silicates allows to form silica formations [10]. Due to the negative surface charges of silica in water at pH 5.8, dispersion of silica spheres tolerates the Pb<sup>2+</sup> ions to get adsorb over it. Finally, the immersing of formed Pb<sup>2+</sup>@Silica in the solution of S<sup>2-</sup> will form the SiO<sub>2</sub>@PbS nanostructures. The crystallinity of the SiO<sub>2</sub> spheres, SiO<sub>2</sub>@PbS core–shell nanoparticles were studied by

XRD. The sharp amorphous peak at  $22^\circ$  indicates the uniformity of silica spheres (Fig. 1) as reported elsewhere [11]. The XRD pattern of synthesized powder for Silica@PbS nanoparticles are shown in Fig. 2. It shows several diffraction peaks at  $2\theta$  values of 25.9, 30.19, 43.1, 50.9, 53.4, 62.5, 70.9, and  $79.1^\circ$ , which correspond to the Miller index of the reflecting planes for (111), (200), (220), (311), (222), (400), (420), and (422). All the diffraction peaks in the spectra are analogous to the literature pattern of face-centered cubic phase PbS powder (JCPDS file no. 5-592), confirming the formation

of PbS nanoparticles. The strong and sharp diffraction peaks suggest that the as-obtained products are well crystallized. The amorphous peak of silica at  $22^\circ$  is not identified in the pattern of the  $\text{SiO}_2$ @PbS. This may be due to complete coverage of silica by the shell layer. No other impurity peaks in the diffraction pattern indicate the purity of  $\text{SiO}_2$ @PbS core-shell system. Further the widened full width at half maximum (FWHM) of peaks in the PbS diffraction pattern indicates the smaller layer thickness [12].

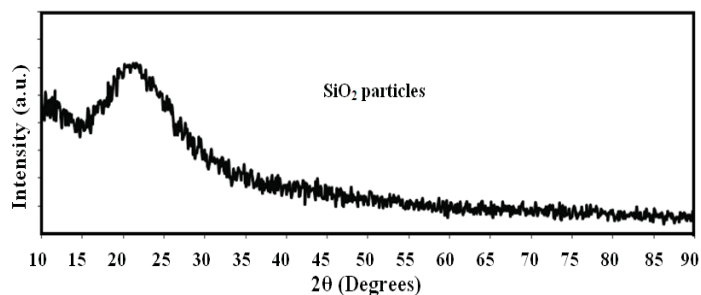


Fig. 1 XRD pattern of  $\text{SiO}_2$

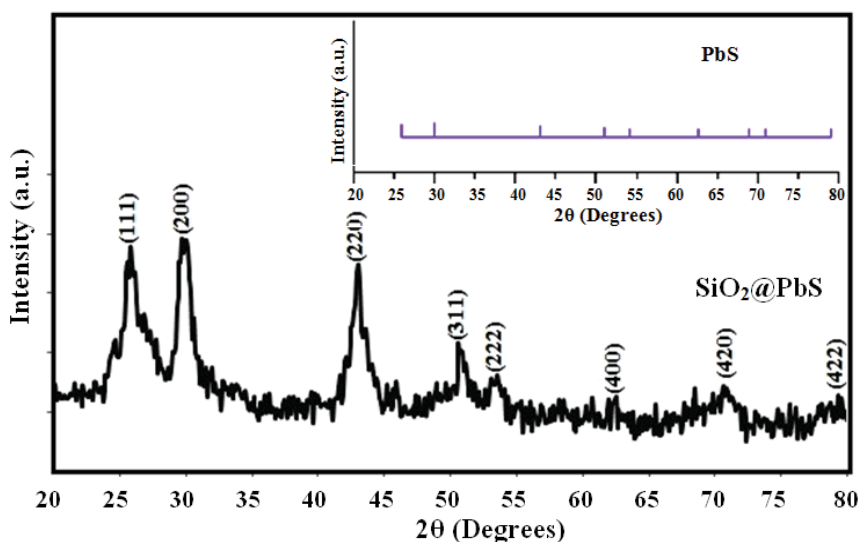


Fig. 2 XRD pattern of  $\text{SiO}_2$ @PbS core-shell (inset: XRD of PbS nanoparticles)

The FT-IR spectrums of these nanostructures are shown in Fig. 3. FT-IR spectrum of silica shows the characteristic vibrations of  $\text{SiO}_2$  and CTAB (Fig. 3 (a)). The vibrations at  $1057$ ,  $791$ , and  $454\text{ cm}^{-1}$  are the respective to Si–O–Si, Si–O, O–Si–O bonds. Vibrations occurred at  $962$  and  $1645\text{ cm}^{-1}$  are for stretching of non-bridging oxygen atoms present in unreacted Si–OH group and weak bending vibration of H–O–H in  $\text{H}_2\text{O}$ . The CTAB can be realized at the wave numbers  $2853$ ,  $2922\text{ cm}^{-1}$  (tail group vibrations), and  $1477\text{ cm}^{-1}$  (head group vibration). The spectrum taken for  $\text{SiO}_2$ @PbS (Fig. 3 (b)) remarked a few noteworthy changes in the observed vibrations of silica particles. The characteristic vibrations of CTAB and  $\text{SiO}_2$  decrease in its intensity, after the PbS layer

formed over the silica. The intensity of N–CH bonding stretching has been reduced, but the intensity of N–H bonding is slightly increased.

SEM images of  $\text{SiO}_2$  particles and  $\text{SiO}_2$ @PbS nanostructures are shown in Figs. 4 (a)–(d). Figs. 4 (a) and (b) show SEM images of  $\text{SiO}_2$  particles. A panoramic SEM image in Fig. 4 (a) demonstrates that the obtained pure  $\text{SiO}_2$  powder shows spherical morphology on a large scale. These spheres are relatively unique in size, with a diameter  $\sim 250\text{ nm}$ . Moreover, high magnification SEM images in Fig. 4 (b) show that the surface of the composite is basically smooth. Figs. 4 (c)–(d) shows the images of the Silica@PbS nanostructures. It can be seen that the sphere surfaces were not as smooth as that

of pure SiO<sub>2</sub>, due to the formation of nanosized PbS particles. The sizes of the SiO<sub>2</sub>@PbS nanostructures are about 300 nm.

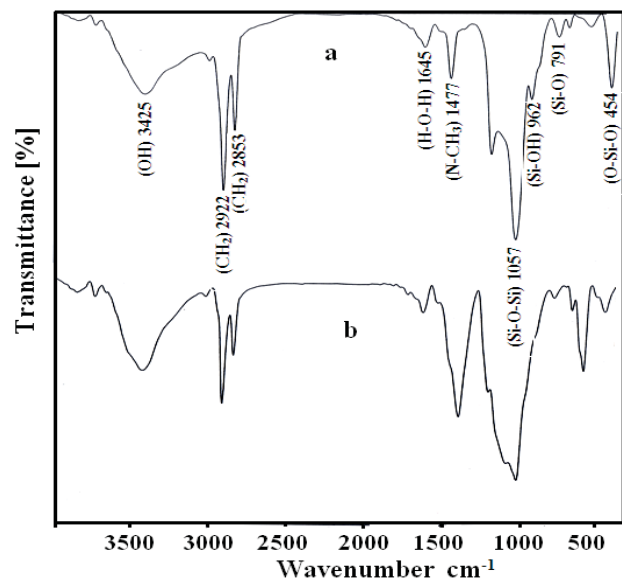


Fig. 3 FT-IR spectra of SiO<sub>2</sub> (a) and SiO<sub>2</sub>@PbS core-shell nanoparticle

The TEM analysis revealed the formation of the core-shell nanostructures (Fig. 5). We observed a grayish layer around the SiO<sub>2</sub> particles and the thickness of the layer was about only 18 nm which indicates the formation of a lead sulphide shell on the particles surface.

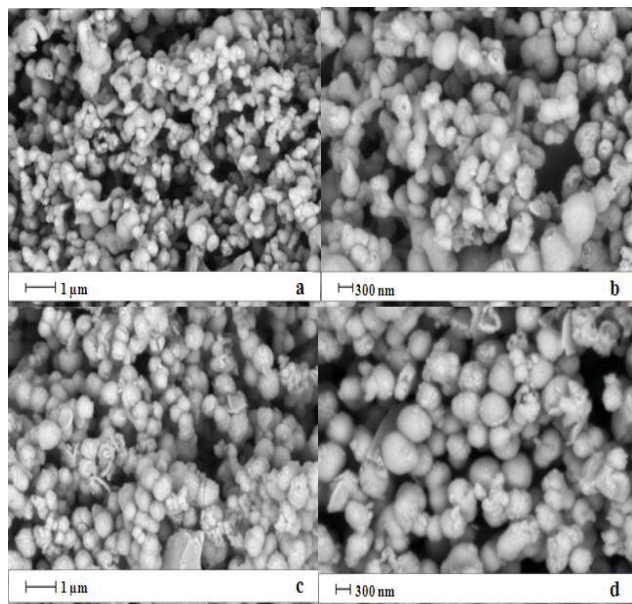


Fig. 4 Low and high magnifications SEM images for the pure SiO<sub>2</sub> particles (a) and (b), and SiO<sub>2</sub>@PbS nanostructures (c) and (d)

The UV-vis diffused reflectance spectrum (UV-vis DRS) for Silica@PbS nanoparticles is shown in Fig. 6. In common

excitonic absorption and emission helps in understanding the purity of the samples and it gives information about the defects present in the crystal system. The bulk PbS gave an absorption at 3020 nm [13]. Comparing the absorption edge of bulk PbS to that of SiO<sub>2</sub>@PbS core-shell, it is seen that a large blue shift in the onset of absorption is observed in this sample. This blue shift indicates that PbS exists as small clusters [6]. This phenomenon of blue shift of absorption edge has been ascribed to a decrease in particle size. It is well known that in case of semiconductors the band gap between the valence and conduction band increases as the size of the particle decreases in the nanosize range. This results in a shift in the absorption edge to a lower wavelength region. The magnitude of the shift depends on the particle size of the semiconductor. In the present study, the Silica@PbS samples prepared from solution showed a blue shift of approximately 2460 nm compared to the bulk particles. The band gap of PbS has been determined as 2.01 eV directly from the absorption maximum of PbS,  $\lambda_{\text{max}} = 560$  nm. The bandgap of the bulk PbS is 0.41 eV. The bandgap edge of PbS gets 1.6 eV blue shifted than bulk PbS, which may be due to quantum confinement. The widened FWHM observed in XRD and morphological analysis also confirming the thinner PbS shell layer.

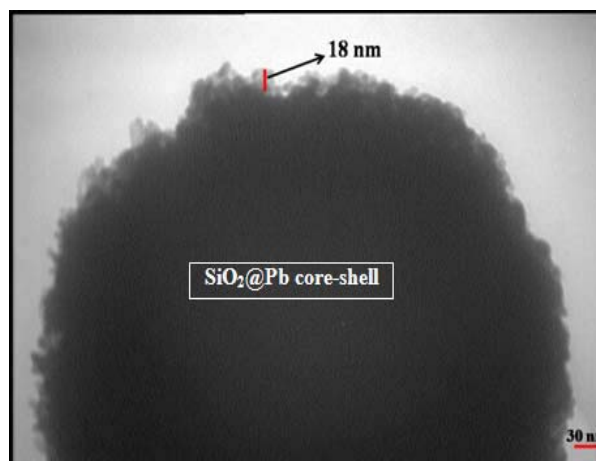


Fig. 5 TEM image of SiO<sub>2</sub>@PbS core-shell nanostructure

#### IV. CONCLUSION

In this paper, we have reported a simple method to synthesize SiO<sub>2</sub>@PbS core-shell nanoparticles at ambient conditions. The results of XRD, SEM, UV-vis, FT-IR and TEM measurements indicate that SiO<sub>2</sub>@PbS nanostructure is synthesized in our experiment. The PbS nanoparticles are crystalline. A large blue shift in the absorption edge was observed in the samples prepared by an ion-exchange method, indicating the formation of nanometer-sized PbS nanoparticles, as a consequence of particle size effects. The silica spheres of ~250 nm and the shell thickness of ~18 nm have been identified in the morphological studies. With this fine thickness, PbS shell layer is exhibiting the peerless optoelectronic behaviors.

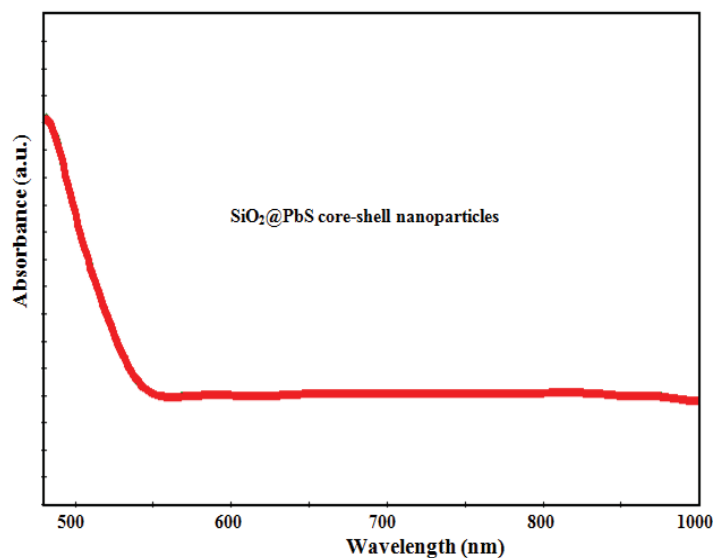


Fig. 6 UV-vis absorption spectrum of SiO<sub>2</sub>@PbS nanoparticle

#### ACKNOWLEDGMENT

Financial support by Rasht Branch, Islamic Azad University Grant No. 4.5830 is gratefully acknowledged.

#### REFERENCES

- [1] Y. Ni, H. Liu, F. Wang, Y. Liang, J. Hong, X. Ma, Z. Xu, *Cryst. Growth Des.* 4 (2004) 759–764.
- [2] Bo Ding, Minmin Shi, Fei Chen, Renjia Zhou, Meng Deng, Mang Wang, Hongzheng Chen, *J. Cryst. Growth* 311 (2009) 1533–1538.
- [3] A. Pourahmad, *Spectrochim ACTA A*, 103 (2013) 193-198.
- [4] Shuling Shen, Qiangbin Wang, *Chem. Mater.* 25 (2013) 1166–1178.
- [5] A. Dementjev, V. Gulbinas, *Opt. Mater.* 31 (2009) 647–652.
- [6] A. Pourahmad, *Mater Lett.*, 65 (2011) 2551-2553.
- [7] R.D. Schaller, M. Sykora, J.M. Pietryga, V.I. Klimov, *Nano Lett.* 6 (2006) 424–429.
- [8] D. Gachet, A. Avidan, I. Pinkas, D. Oron, *Nano Lett.* 10 (2010) 164–170.
- [9] D. Wang, J.K. Baral, H. Zhao, B.A. Gonfa, V.V. Truong, M.A. El Khakani, R. Izquierdo, D. Ma, *Adv.Funct.Mater.* 21(2011)4010–4018.
- [10] R.I. Nooney, D. Thirunavukkarasu, Y. Chen, R. Josephs, A.E. Ostafin, *Chem. Mater.* 14, (2002) 4721-4728.
- [11] Y. Kievsky, I. Sokolov, *IEEE Trans. Nanotechnol.* 4, (2005) 490-494.
- [12] W. Tang, F. Teng, Y.B. Hou, Y.S. Wang, F.R. Tan, S.C. Qu, Z.G. Wang, *Appl. Phys. Lett.* 96, (2010) 163112.
- [13] F.W. Wise, *Acc Chem Res.* 33 (2000) 773-780.